A prefrontal source of visual target enhancement in the macaque area V4

Azriel Ghadooshahy

B.S. Cybernetics
University of California at Los Angeles, 2008

SUBMITTED TO THE DEPARTMENT OF BRAIN AND COGNITIVE SCIENCES IN PARTIAL FULLFILLMENT OF THE REQUIREMENTS FOR THE DEGREE OF

MASTER OF SCIENCE IN NEUROSCIENCE
AT THE
MASSACHUSETTS INSTITUTE OF TECHNOLOGY
JANUARY 2017

[February 2017]

Signature of Author: Signature redacted
Department of Brain and Cognitive Sciences
January 20th 2017

Certified by: Signature redacted
Robert Desimone
Doris and Don Berkey Professor of Brain and Cognitive Science
Thesis Supervisor

Accepted by: Signature redacted
Matthew A. Wilson
Sherman Fairchild Professor of Neuroscience and Picower Scholar
Director of Graduate Education for Brain and Cognitive Sciences

A prefrontal source of visual target enhancement in the macaque area V4

By

Azriel Ghadooshahy

Submitted to the department of Brain and Cognitive Sciences on January 20th, 2017, in partial fulfillment of the requirements for the degree of Masters of Science in Neuroscience.

ABSTRACT

The ventral pre-arcuate area (VPA) in the primate prefrontal cortex has recently been found to play an important role in feature-based selection of visual targets in the context of a naturalistic free-gaze visual search task. While VPA neuronal activation was found to be necessary for behavioral performance as well as target selection in the FEF, its role in the broader context of the visual system remains to be addressed. To this end, we have interrogated the role of the VPA in mediating the effects of feature attention in the macaque visual area V4 by recording in V4 with and without muscimol inactivation in the VPA. We report here that neuronal activation in the VPA is necessary for firing rate increases related to target selection in V4.

KEYWORDS: feature attention, visual search, muscimol, neurophysiology

Thesis Supervisor: Robert Desimone
Title: Doris and Don Berkey Professor of Brain and Cognitive Science

TABLE OF CONTENTS

INTRODUCTION

Feature-based visual search is represents a critical behavioral capacity in higher primates and a key model paradigm for studying the neural basis of executive function. Previous studies from our group have shown that in rhesus monkeys performing visual search, V4 neurons responded more vigorously to the presence of cued vs uncued stimuli and that the effect of attention is increased for preferred versus non-preferred stimuli under specific experimental conditions[1]. Subsequently it was shown that target enhancement, as well as share-color and share-shape stimuli were enhanced by attention and that selection occurred earlier in the frontal eye fields (FEF) than in visual area V4, which strengthened the working model of an FEF "salience map" as well as highlighted a neural circuit comprising top-down feedback to V4 via the FEF[2,3]. However it is also known that FEF neurons are not intrinsically stimulus selective, and thus cannot be the primary source of feature attention and featured-based target-selection observed in the FEF, as well as V4. Thus, Bichot *et al* hypothesized that another nearby region on the gyrus immediately anterior to the FEF, with neurons exhibiting intrinsic object preferences, might be the source of this target-object enhancement observed in FEF. They denoted this region as the ventral pre-arcuate area (VPA) and showed that VPA activation is necessary for target selection in the FEF, highlighting the important role of the VPA in the "what" visual pathway as a part of a broader circuit including the principal sulcus and inferotemporal cortex (IT)[4]. However, a critical test of the FEF salience map and V4-FEF-VPA macrocircuit models is whether or not VPA activation is necessary for target enhancements in V4, as well as potentially the share-color and share-shape enhancements[2].

To address these questions, as well as clarify the role of the VPA in the broader context of visual feature and object attention, we recorded in the macaque visual area V4 with and without muscimol inactivation in the VPA during free-gaze visual search.

RESULTS

Monkeys were trained to perform a free-viewing visual search task with a stimulus set consisting of conjunctions of 7 shapes and 7 colors ("Search7s7c"), as well as two fixation tasks including an RFMAP task and feature mapping tasks (see methods). The RFMAP task was used to estimate the appropriate settings for the search array, with the intention of placing a given recorded V4 site at specific array location (**Fig.2B**). The feature mapping task was used to measure neuronal stimulus preferences in the absence of pre-cueing (e.g. 'intrinsic preferences') in order compute marginal feature preferences based on the same stimulus set that was used in the search task (e.g. 'selection preferences' related to attention), as well as provide a point of reference for interpreting the effects of VPA muscimol in the V4 firing rate. For the Search7s7c task, the animals were presented with a central cue object that was the target of the visual search when presented among distractor objects after a delay period (**Fig. 1**). No restrictions were placed on monkeys' search behavior other than they had to fixate the target object for a prescribed duration continuously in order to register a correct response and receive reward. On each trial, one of a fixed set of 20 objects was pseudorandomly selected online from the master list of 49 possibilities as the cued target, then two share shapes and two share colors as well as 15 no-share distractors were selected and assigned to the remaining locations. For a complete session, each stimulus would be presented at each location exactly once for a total of 20x49 = 980 trials plus 10x detections at each location for an additional 200 trials. The detection stimulus was a luminance-matched gray square stimulus presented alone at any of the array positions which had no features in common with the search stimulus set, and these trials were used to check the spatial localization of recorded channels (see methods) and to assign the most suitable array location index to a given multiunit for analysis.

In this report, we are specifically addressing firing rate effects measured at array onset during the search task, which occurred at the end of the delay period in the search task (**Fig.1**). The reason for emphasizing this time point versus subsequent saccades is that the task design and balancing across stimulus presentations at recorded RFs is experimentally controlled for array onset and less so for secondary saccadic behavior. Due to trial count limitations and other practical considerations based on pilot studies, we opted for an unpaired design in which V4 for recordings made with VPA muscimol injections and control recordings, and special effort was made to collect data in a 'psuedo-paired' fashion by keeping the recording locations in V4 for pairs of muscimol and control sessions consistent.

Effects by condition in V4

In order to quantify baseline effects of attention, we measured firing rate differences in V4 with respect to cueing conditions. We considered stimulus categories including target, no-share, share-shape and share-color and measured attention as the difference between no-share and the other conditions. In order to address spatial versus feature enhancement effects, we considered separately cases in which the monkeys would make a saccade into a given receptive field versus away. Saccade-IN cases were

those in which an RF stimulus response was measured and the monkey subsequently made a saccade to the corresponding array location, and saccade-OUT cases were measured for stimuli given that the monkey would subsequently look at some location that is not in the array location corresponding to its RF. Thus, we measured the effects of featured-based V4 neuronal selection by considering the difference in firing rate modulation between attended conditions (target, share-shape, or share-color) and the non-attended no-share condition for saccade-OUT cases. Saccade-IN cases were used to measure spatial selection in V4, which we do not expect to decrease with muscimol in the VPA based on the findings of Zhou and Desimone (2011) and Bichot *et al* (2015) by taking all saccade-IN vs saccade-OUT trials (collapsed across cueing conditions) from a given session.

Response measurements for target, share-shape and share-color effects on neuronal selection in the firing rate were performed by computing the average percent change (e.g. [A-B]/B) bin-by-bin between the no-share response trace and that of each of the attended conditions measured at the array onset. For spatial selection we measured the mean percent change between saccade-IN and saccade-OUT conditions. Primary effects of attention and spatial selection were tested with t-tests against the zero-mean null hypothesis. The results of the t-tests are shown in the top right of the percent change population histograms for each condition and each monkey (**Fig. 3B, 4B**, for target selection; **SuFigs 1B, 2B, 3B and 4B** for share conditions). We observed significant firing rate increases in the response period for both target (ttests, $p < 0.001$ for each) and spatial selection (ttests, $p < 0.05$ and $p < 0.01$, respectively) in each monkey under control conditions. In separately recorded (unpaired design) sessions with muscimol injections in the VPA, a small but significant decrease in the target selection effect for monkey #1 (ttest, $p < 0.05$) and there was no effect of neuronal target selection in monkey #2 (ttest, $p > 0.05$). The neuronal V4 spatial selection effect appears to remain intact for both monkeys (ttests, $p < 0.05$ for both).

Effects of feature tuning in V4

Attentional processes in V4 are known to interact with intrinsic stimulus preferences in the context of V4 recordings, and it has been previously observed that the effect of attention is increased when cued features presented in the RF are preferred relative to non-preferred. Here we addressed the possibility that intrinsic *feature* preferences play a role in modulating observed general effects of attention in the firing rate by computing marginal responses to features along color and shape dimensions measured in the feature mapping task. We tested for a systematic relationship between measured effects of attention and intrinsic feature tuning by conditioning our analysis of attention by condition and feature on the rank-ordered indices for each feature dimension obtained from feature mapping data. That is, we sorted the mean firing rate responses to each of the 7 shapes (collapsed across colors) and 7 colors (collapsed across shapes). By rank-ordering the feature responses, we obtain indices to the same features, computed from responses measured with the same set of stimuli as the search task (PrIDX, see methods). We tested whether the feature-mapped preferences were predictive of V4 target selection responses during search, and also considered the rank-ordered feature responses based on noshare responses

(FsIDX; see methods). For both, we computed the difference of the mean firing rate responses for target vs noshare, shareshp vs noshare, and sharecol vs noshare with separate normalizations for each binary comparison (see methods). We tested for effects of feature index, feature dimension and condition (targ-noshare, sharecol-noshare, noshare-noshare). For the FsIDX measurements (**Fig.7A**) we found a significant two-way interaction between index and condition (monkey 1, $p < 0.05$) as well as the three-way interaction between index, condition and feature dimension (monkey 1, $p < 0.05$). For the PrIDX measurements, the ANOVA returned no significant effects in either monkey (**SuFigs.5,6**).

Effects of VPA inactivation on attention in V4

The key prediction of our study was that VPA inactivation would selectively ablate positive effects of attention (e.g. target selection) in the V4 firing rate while sparing saccadic (spatial) effects related to saccades into the RF (e.g. spatial selection). Thus we tested the hypothesis on the set of mean percent differences (histogram data, **Figs 3AB, 4AB**) using a two-way ANOVA with an unpaired design with factors for muscimol (VPA inactivated or not) and selection type (target selection vs spatial selection), separately for each monkey, yielding a significant result on the main effect of muscimol in monkey #1 ($p = 0.001$) and a nearly significant for the muscimol x selection interaction for monkey #1 ($p = 0.054$). However, ANOVA tests were not significant for monkey #2, perhaps due to small N after attrition from low-trial count rejections as well as detection processing rejections (which were especially prevalent for one monkey #2 inactivation session in particular).

Effects VPA inactivation on behavior

We also analyzed the effect of VPA muscimol on general aspects of first-saccade behavioral choices in terms of visual field quadrant and stimulus category (target, share-shape, share-color, no-share; **Fig.9, Fig.10**). Here we performed hypothesis testing on a session-basis and given relatively few sessions overall across both monkeys (many channels recorded, only one measurement per session for behavior), we therefore performed single tests on the combined behavioral data from both monkeys.

Regarding first choice saccade quadrant data, note that the first saccade quadrant behavioral data and the associated changes under muscimol inactivation (**Fig.10B**) are idiosyncratic due to the relationship between default behavioral patterns observed in first-saccade choices for each monkey and the hemisphere in which injections and recordings were done. Specifically, monkey #1 was implanted with chambers on the left hemisphere and displayed a spatial bias on the first saccade towards the left visual hemifield (and more specifically, top left), while monkey #2 also showed a bias towards the left visual hemifield (see **Fig.10A-B**, "TL" bars) but was implanted in the right hemisphere, which results in VPA inactivation effects in the left visual hemifield, thusly resulting in a strong spatial effect of VPA muscimol on the initial saccade direction (by quadrant) in monkey #2 and apparently little effect in monkey #1. Accordingly, a 3-way ANOVA with an unpaired design by quadrant, muscimol and

monkey revealed significant primary effects of muscimol ($p < 0.01$) and monkey ($p<10^{-14}$), as well as a significant interaction between muscimol and monkey ($p < 10^{-10}$).

For categorical choices, there was an apparent decrease in the probability of behavioral target selection for the first saccade (**Fig.9, Fig.10; C** vs **D**). We performed a two-way ANOVA with an unpaired design by stimulus category and VPA inactivation. We found in these behavioral data that there was a significant primary effect of stimulus category ($p < 0.001$) as well as a significant interaction between category and inactivation ($p < 0.05$), with a non-significant primary effect of VPA inactivation.

DISCUSSION

It is interesting and slightly unexpected that share-color effects may remain intact under VPA muscimol inactivation conditions (**SuFigs 2,4**), especially given the apparent share-color-based strategy observed in both monkeys (**SuFig 7**) as well as the informal observation that muscimol-induced behavioral deficit in target selection appears to be associated with a concomitant increase in the frequency of share-color behavioral selections (**Fig.9C,D, Fig10,C,D**). The apparent lack of effect on share-color enhancement suggests that this enhancement may be mediated by mechanisms that are different than those supporting the target enhancement effects that were specifically ablated by VPA muscimol inactivations. We also found a consistent 2nd order effects of muscimol in the feature-resolved analysis, indicating that on the observed positive enhancements seen in the control feature-resolved datasets were selectively modulated by VPA inactivation while the apparent negative aspects were spared (**Fig.7,8**). Moreover, we found that intrinsic feature tuning measured outside of the context of the task was not predictive of the observed selection tuning, and based on the current analysis, therefore, is unlikely to confound our interpretation of the effects of VPA muscimol inactivation on general measures of target enhancement in the V4 firing rate. Lastly, we found specific behavioral deficits in both monkeys that were highly consistent with VPA inactivations and highly consistent with our hypothesis that VPA neuronal activity is necessary for behavioral target selection (**Fig.9,Fig.10**). A more detailed treatement of secondary saccadic behavior and firing rate effects is pending and will be included in a future revision of this manuscript.

We recorded in the area V4 of rhesus monkeys while inactivating their prefrontal VPA during free-gaze visual search. We found that under control conditions, there were strong effects of target selection as well as spatial selection, establishing our baseline conditions of attention measurements in V4. When muscimol was injected in VPA, neuronal target selection in V4, as well as behavioral target selection, were greatly reduced while neuronal spatial selection in V4 was (nominally) spared and general behavioral patterns in terms of spatial choices (**Fig.9A,B, Fig.10A,B**) and color-based strategy (**SuFig.7**) remained relatively constant. Moreover, given the interaction effects in the tuning analysis and selective reduction of behavioral target selection, we note the consistency with the notion that VPA may mediate feature *conjunction* processing underlying neuronal target selection in V4. Thus, we conclude that VPA is a necessary source of top-down input to V4 (likely indirectly via FEF).

METHODS

Subjects and surgical procedures. Two rhesus monkeys weighing 8-16 kg were used. The animals were cared for in accordance with the National Institutes of Health Guide for the Care and Use of Laboratory Animals and the guidelines of the MIT Animal Care and Use Committee. All surgical procedures were carried out under anesthesia, and animals received antibiotics and analgesics after surgery. Under aseptic conditions, monkeys were implanted with a headpost and chambers that allowed access to brain regions for neural recording and inactivation.

Behavioral tasks.

Control system. The experiments were under the control of a PC computer using MonkeyLogic software (University of Chicago, IL), which presented the stimuli, monitored eye movements, and triggered the delivery of the electrical or fluid reward. Monkeys were seated in an enclosed chair and their eye position was monitored using an EyeLink II or EYESCAN infrared, video-based system (SR Research Ltd., Ontario, Canada). Stimuli were presented on an LCD video monitor (Dell Ultrasharp U2401 with 120 Hz, 1920x1440 resolution) viewed binocularly at a distance of 57 cm in a dark isolation box (Crist Instrument Co., MD).

RF mapping task – In each session a simple passive fixation task in which white boxes subtending 1dva were randomly presented at a discrete and nonoverlapping set of locations spanning 10 visual degrees from fixation on a fixed grid. By computing the response at each location we constructed heatmaps visualizations of the RF on a given channel which guided the online placement of the search array for that session.

Feature mapping task – In each session after mapping RF coordinates, we also mapped the passive feature preferences by briefly presenting (100ms) the stimuli used in the search task at the RF as well as 4 other control locations that were rotated 90 degrees from the indicated RF location in order to avoid introducing possible systematic spatial biases in the behaving subjects. Each stimulus from the stimulus set was presented 5-10 times depending on the session.

Search task – The stimuli used in the search task comprised a 7x7 set of shape-color conjunctions. The images that were matched for the number of pixels different from background, and subtended an area of approximately 1.5x1.5 dva with a 2:1 contrast ratio. On each trial, a pseudorandomly generated subset of twenty stimuli were selected starting from the target, and then ensuring a constant proportion of 2 items that share the shape of the target and 2 items that share the color of the target, in addition to 15 non-share cases. Arrays conditions were generated online, trial-by-trial using built-in MATLAB randomization function including randi. After fixating a small, white central fixation point for 800ms, either a white square was presented for a detection trial, or a central cue informed the subject of the target stimulus on that trial. The cue stimulus was presented for 1000ms, after which time it was extinguished and replaced by the fixation spot for another 800ms. Subjects were required to hold fixation at the center of the screen during this delay period. At the end of the delay period, the fixation spot was extinguished and the array appeared which signaled the monkey to begin searching for the remembered target. In order to register a correct response, the monkeys were required to fixate the target stimulus for 800 ms continuously before receiving a juice

reward. For search trials, the animals had 5s from search array onset to find the target, and no constraints were placed on their search behavior in order to allow them to conduct the search naturally. For detection trials, the animals had 500 ms to enter the target window and keep fixation at the target location until. The inter-trial interval was 1 s.

Recordings. Multiunit recordings were conducted using multi-contact laminar probes (V-probes, Plexon Inc., Dallas, TX). Each probe had 16 contacts spaced 150 um apart. The electrodes were advanced manually using custom-made screw mini-microdrives mounted on a plastic grid (**SuFig.11**). Neural signals were amplified, band-pass filtered, and digitized using the Omniplex system (Plexon Inc). In addition, a grid system was used inside the recording chambers to guide electrode penetrations and localize them relative to structural MRI images (MPRAGE, 500 um isotropic). Penetration locations were confirmed with gray to white matter transition depths. Ventral pre-arcuate (VPA) recording sites were on the pre-arcuate gyrus, approximately 2-4 mm anterior to the arcuate sulcus and ventral to the principal sulcus, and the penetrations did not enter either the arcuate sulcus or the principal sulcus (i.e., white matter was reached by the expected depth). Area V4 recordings were located anterior to the lunate sulcus, posterior to the superior temporal sulcus (sts) and superior to the inferior occipital sulcus (ios).

Inactivations. Muscimol (5ug/ul) was injected in at previously RF mapped VPA recording sites *intended to inactivate in the entire contralateral hemifield covering search array locations*. This is in contrast to a design aimed at more spatially restricted inactivations like the data seen in **SuFig.9.** In a given session, we made injections of 1ul at two different depths and two locations within the area. The injections started at the deeper location first, and the second injection was made by retracting the cannulas by steps of ~1mm. The injections were made at a rate of 0.05 ul/min with a 5-minute wait between injections, and data collection began 45min-1h after the final injection.

Data analysis. All analyses were done using custom-written software in MATLAB (Natick,MA).
Firing rate calculations – Spike densities for each multiunit were computed directly from spike times with 40khz temporal resolution by computing the instantaneous firing rate *IFR = 1 / (t{i+1} – t{i})* for each trial, averaging the single-trial densities, and then convolving with a 10ms boxcar for smoothing. For population analysis of binary comparisons between conditions (e.g. target vs noshare), raw firing rate densities were normalized to max(max(a),max(b)) in order to be passed along for response measurements and population analysis.
Spatial localization test – Recording with V-probes in V4 generally yielded consistent RF locations across contacts such that the RF corresponded to the same array location for each channel. However there were cases in which some RFs were not spatially well-localized to a single location or showed preferred spatial responses on detection trials at a nearby array position. Thus we implemented a procedure to screen multiclusters for analysis based on whether or not they have detection responses that are reliably associated with a single array position, and we used the strongest sorted response from

detection trials to automatically assign the array position to a given cell for analysis since in rare cases the nominal cross-channel location (based on visual inspection of RF maps) was different, and the outcomes were verified manually by graphical inspection. Cells were rejected if they failed to show a significant primary effect of position in a one-way ANOVA (which would imply that we cannot distinguish responses at different locations in general), and were also rejected if the first and second sorted responses were not significantly different according to a post-hoc multiple comparisons test at a confidence level of 0.05. In other words, when the top two sorted detection responses are statistically indistinguishable, we cannot confidently attribute the response measurements on a given channel to a single array location and thus the datapoint in question is unsuitable for the analyses presented in this paper.

Tuning analyses – In order address potential effects of intrinsic stimulus preferences on our measurements of attentional effects in V4, we considered two different approaches to quantifying the effects of individual features on measurements of attention. First we computed the tuning curve measured from the feature mapping task by constructing spike densities for each feature along each feature dimension, and ranking the responses to the obtained sorted indices. These marginal densities were computed for each feature along each dimension (shape and color) and collapsed across the other dimension, using the stimulus set which was used in the search task. For example, a color tuning curve is computed by measuring the spike density response to all presentations of a given color (e.g. all red stimuli) regardless of shape. In the first approach, we used feature-mapping data and refer this as "preference indexing" or PrIDX in some figures, and we similarly computed a "selection index", abbreviated as FsIDX, by instead ranking the feature responses from the noshare condition at array onset.

Statistical analyses – Hypothesis tests were performed using built-in MATLAB functions including *ttest*, *anovan* and *multcompare*.

REFERENCES

1. Bichot, N.P., Rossi, A.F. & Desimone, R. Parallel and serial neural mechanisms for visual search in macaque area V4. *Science* **308**, 529-534 (2005).
2. Zhou, H. & Desimone, R. Feature-based attention in the frontal eye field and area V4 during visual search. *Neuron* **70**, 1205-1217 (2011).
3. Thompson, K.G. & Bichot, N.P. A visual salience map in the primate frontal eye field. *Progress in brain research* **147**, 251-262 (2005).
4. Bichot, N.P., Heard, M.T., DeGenarro M.E. and Desimone, R. A source of feature-based attention in the prefrontal cortex. *Neuron* **308**, 529-534 (2015).

FIGURES TEXT

MAIN FIGURES

Figure 1. Schematic representation of the Search7s7c task. Dotted circles represent the current point of fixation. In the second panel, either a central cue or a peripheral detection target is presented, and if it is a cued (search) trial then there is a fixed 800ms delay before array onset. In this paper we specifically analyze effects measured at the array onset because this is when conditions are most well-balanced and controlled. In this example, the subject made two saccades on his way to correctly identifying the cued target stimulus, the red triangle. Diagrams not drawn to scale.

Figure 2. (A) Schematic representation of brain regions of interest in this study. Note that the VPA is found in the gyrus immediately anterior to the FEF sulcus. For the data presented here, we recorded in V4 and injected muscimol in VPA at locations guided by VPA RFMAP data from previous sessions. (B) An example of an RF heatmap measured using the RFMAP task and rendered from a set of 16 V-probe channels. This heatmap represents the average RF across contacts ("RF composite") from that session, and shows the search array locations used for the session overlaid in red markers. These diagrams are useful for guiding placement of search arrays online, accurately.

Figure 3. V4 firing rate effect of target selection at array onset under control and muscimol conditions. Note that the bar in A and B indicates the response window used for measuring firing rate effects, and the dotted trace represents the population mean differential between the population traces above, which is not the same as the population mean of the individual percent change measurements (mu) indicated in the histograms C and D, and which were the measurements used for hypothesis testing. Error bars represent SEMs.

Figure 4. V4 firing rate effect of target selection at array onset under control and muscimol conditions for monkey #2. Note that N is particularly small in Monkey #2-musc because there were many rejections based on detection processing. Error bars represent SEMs.

Figure 5. V4 firing rate effect of spatial selection at array onset under control and muscimol conditions for Monkey #1. Note that N is smaller because we imposed a 10 trial minimum for analyzing the spatial selection effect as fewer than that tends to be unreliable. Error bars represent SEMs.

Figure 6. V4 firing rate effect of spatial selection at array onset under control and muscimol conditions for Monkey #2. Note that N is particularly small in Monkey #2-musc because there were many rejections based on detection processing. Error bars represent SEMs.

Figure 7. Feature-resolved V4 firing rate effects plotted separately for feature dimension, condition using feature selection indexing based on no-share feature

responses. Control data for Monkey #1 on the left, muscimol data on the right. Error bars represent SEMs.

Figure 8. Feature-resolved V4 firing rate effects plotted separately for feature dimension, condition using feature selection indexing based on no-share feature responses. Control data for Monkey #2 on the left, muscimol data on the right. Error bars represent SEMs.

Figure 9. First saccade behavioral summary data related to spatial and categorical choices, data from Monkey #1. TR = "Top Right", TL = "Top Left", BL = "Bottom Left" and BR = "Bottom Right". TG = "Target", NS = "No-share", SS = "Share-shape" and SC = "Share-color". (A-B) Note that in monkey #1, muscimol injections were in the left hemisphere which induces a scotoma in the right visual hemifield. Note the change in BR saccade probability. (C-D) Note the change in target choice probability. Error bars represent SEMs on session averages.

Figure 10. First saccade behavioral summary data related to spatial and categorical choices, data from Monkey #2. (A-B) Note that monkey #2 was injected in the right hemisphere VPA which induces a scotoma in the left visual hemifield. Note the large difference in TL saccade probability. (C-D) Note the change in target choice probability. Error bars represent SEMs on session averages.

SUPPLEMENTARY FIGURES

SuFig 1. V4 firing rate effect of share-shape selections at array onset under control and muscimol conditions for Monkey #1. Error bars represent SEMs.

SuFig 2. V4 firing rate effect of share-shape selections at array onset under control and muscimol conditions for Monkey #2. Error bars represent SEMs.

SuFig 3. V4 firing rate effect of share-color selections at array onset under control and muscimol conditions for Monkey #1. Error bars represent SEMs.

SuFig 4. V4 firing rate effect of share-color selections at array onset under control and muscimol conditions for Monkey #2. Error bars represent SEMs.

SuFig 5. Feature-resolved V4 firing rate effects plotted separately for feature dimension and condition using feature preference indexing based on data from the feature mapping task. Error bars represent SEMS on session averages. Data for Monkey #1.

SuFig 6. Feature-resolved V4 firing rate effects plotted separately for feature dimension and condition using feature preference indexing based on data from the feature mapping task. Data for Monkey #2. Error bars represent SEMs on session averages.

SuFig 7. Categorical choices plotted as a function of saccade index within trial. Note that there are fewer data points for higher saccade indices, and thus higher variance. Error bars represent SEMs on session averages.

SuFig 8. (left) Over several sessions we were able to detect evidence for a visual topography in the VPA pilot mapping data, which had not been clear in the study by Bichot et al (2015). The 4 sites shown are separately recorded putative VPA sites located near boundaries of the presentation screen aperture recorded during the RF mapping task in monkey #1. There was also one recording which, based on an MRI reconstruction of the grid position, was in the FEF (not shown) and which was foveal but not the same location as the putative foveal VPA site (center green star). **(right)**. In one injection session we injected at two depths at a single site with a recording electrode in order to probe the time-course and specificity of muscimol inactivations.

SuFig 9. (left) In this session the recorded VPA channels showed RFs consistently in the top right quadrant RFMAP, and the array for that session is overlayed on the RF composite for the recorded VPA channels. **(right)** A simple behavioral analysis of reveals a pattern of fixation dwell time consistent with a top-right (TR) VPA inactivatio-- a direct hit, it would seem. However, before exploring any more specific patterns of inactivation it is critical to selectively knock down the entire right visual hemifield, which has been particularly useful in guiding the placement of injection cannulae in monkey #1.

SuFig 10. During the same session, routine screenshots taken for monkey #1 sessions reveal a crude sense of the anatomical scale and time course of muscimol effects in VPA. A single 1uL injection spans about half of the contacts on the 150um spaced contacts, and effects are evident by 30 minutes and more complete by 90 minutes. A recording session aimed at probing the time course of VPA inactivation in V4 and on behavior have not yet been conducted.

SuFig 11. Schematics of a new custom screw drive. Over the course of working on this project, AG (together with Jose @ BCS CNC) designed a specialized screw drive system to improve recording resolution, density and flexibility in both V4 and VPA. Many adjustments were introduced to protect delicate v-probes such as increase lateral stability of shuttles by adding extra shuttle holes, which act as "feet". (A) The original grid pattern with the new one overlayed. One design emphasizes coverage while the other emphasizes resolution and precision positioning, which was instrumental in detecting topographically consistent RFMAP sites due to a rapid magnification in the putative VPA with up to 3 V-probes in one session, as well as performing 2-probe recordings in V4 which helped improve the data yield in monkey #1, although also lead to a higher incidence of detection processing rejections (data not shown). (B) By placing screw holes outside of the recording area we can maximize the access to grid locations in a particular area or location within an area. A binary and complementary shuttle system can be used to configure and interleave shuttles flexibly and closely, and a hex nut at the top with a enough distance from guide holes to allow for a small socket sock wrench to be used for turning, rather than a finicky miniature Phillips screw driving mechanism. (C) An example configuration with multiple shuttles showing the guide holes with tubes representing possible locations for v-probes and/or supporting legs.

FIGURES

MAIN FIGURES

Figure 1.

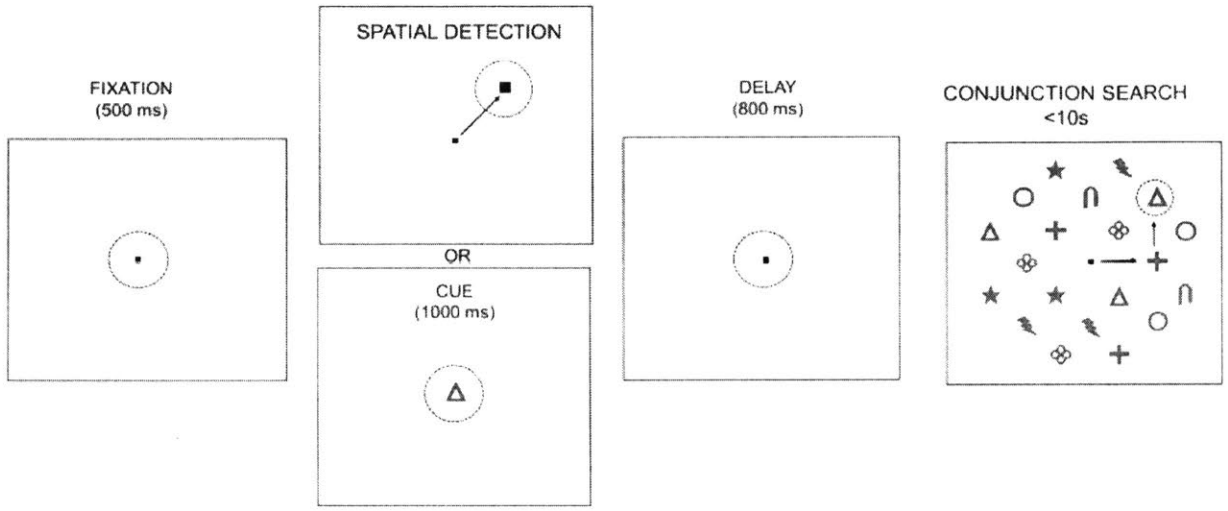

Figure 2.

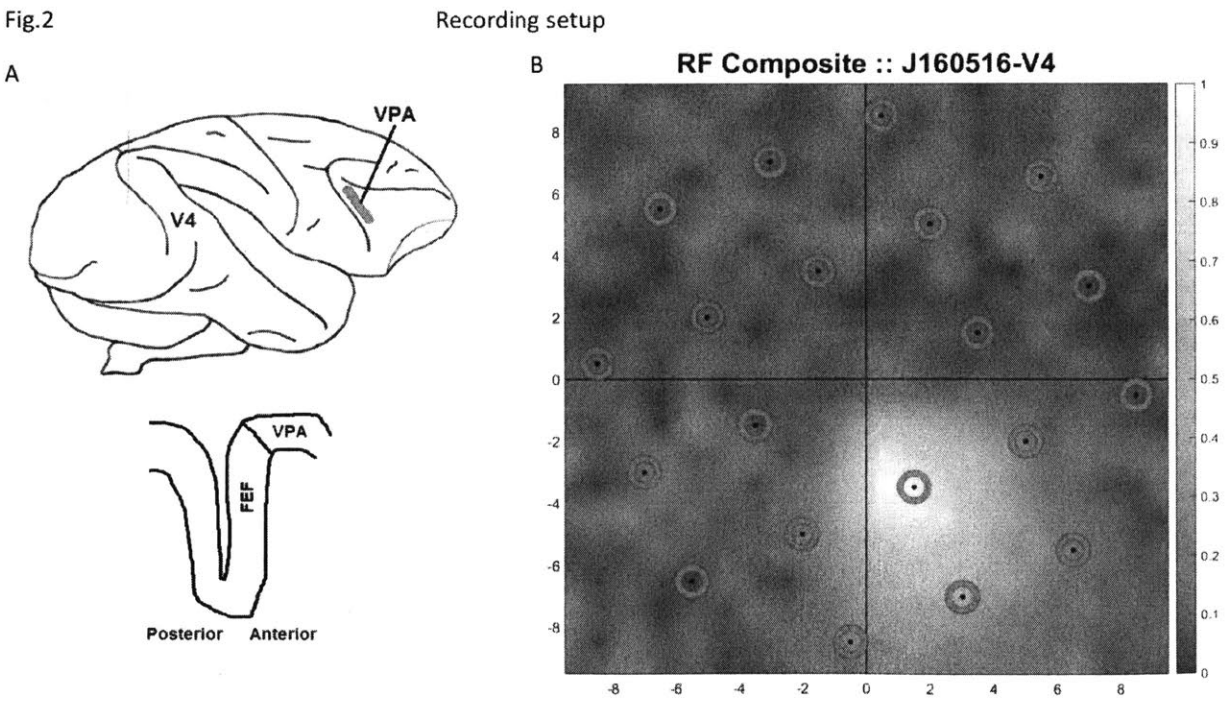

Figure 3.

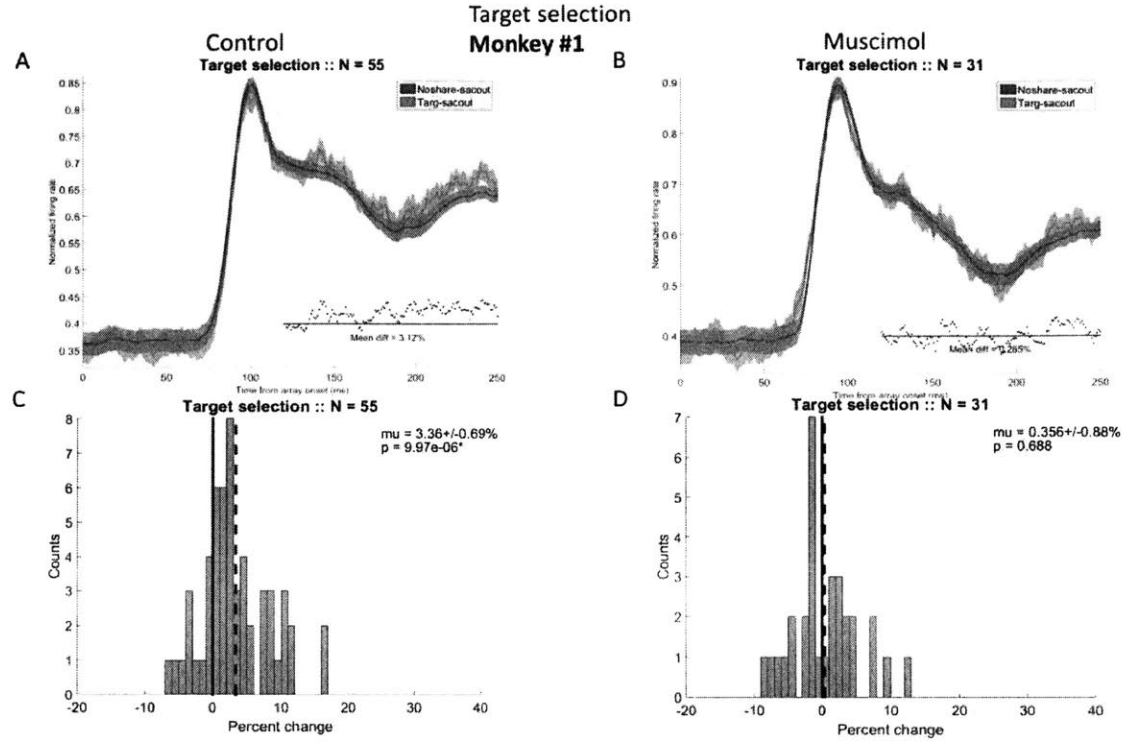

Figure 4.

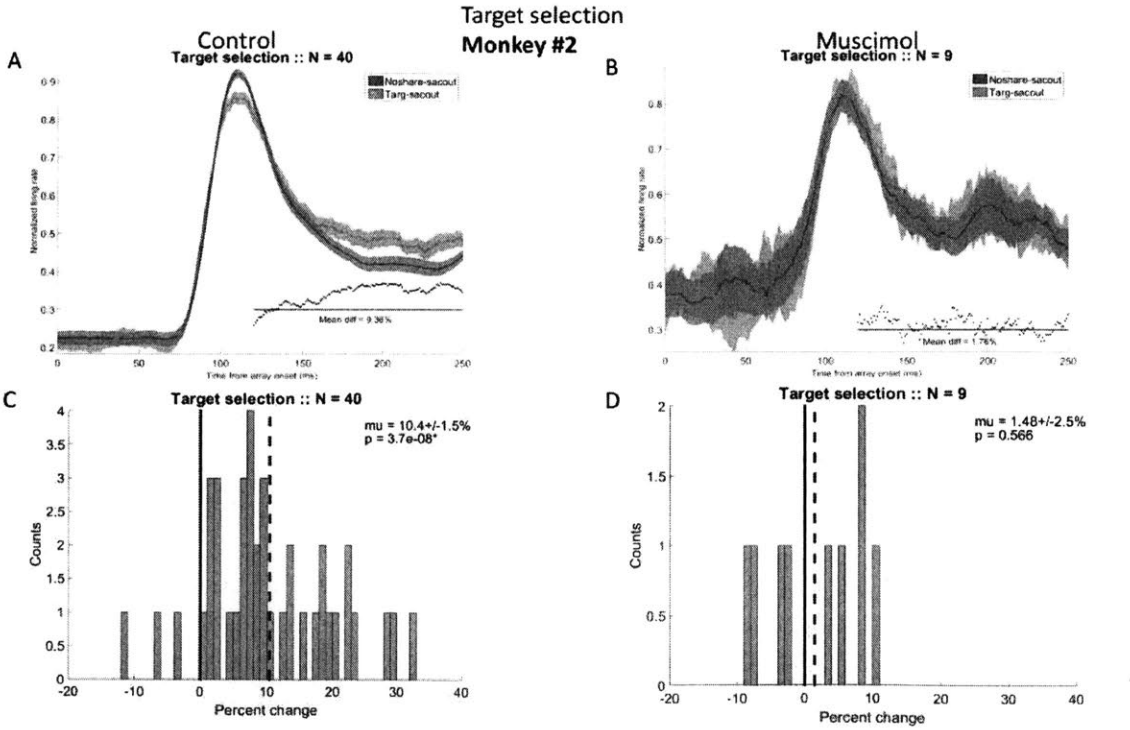

Figure 5.

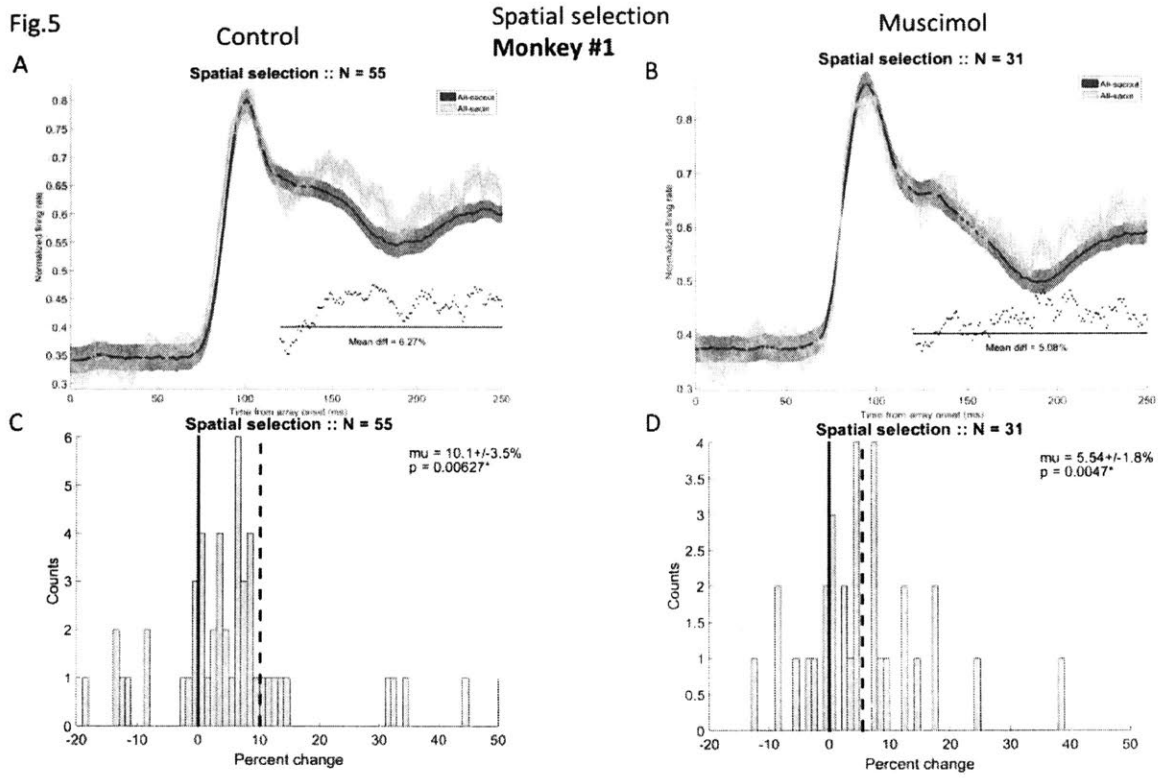

Figure 6.

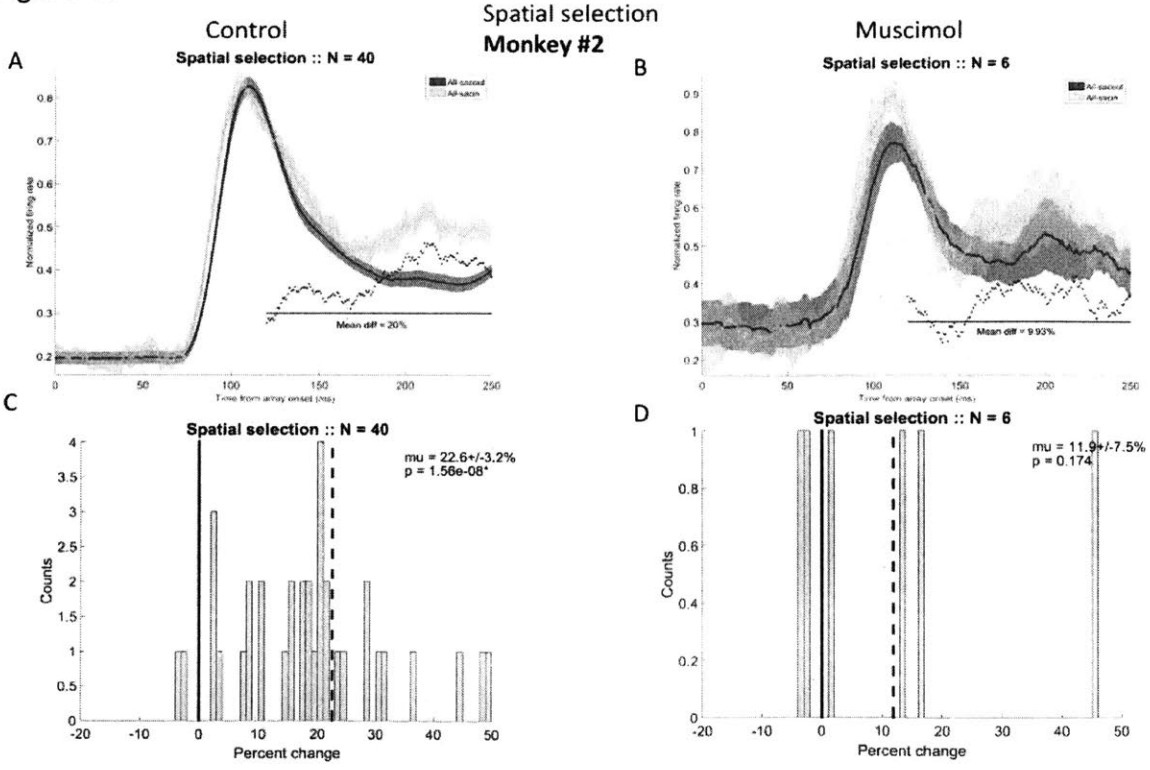

Figure 7.

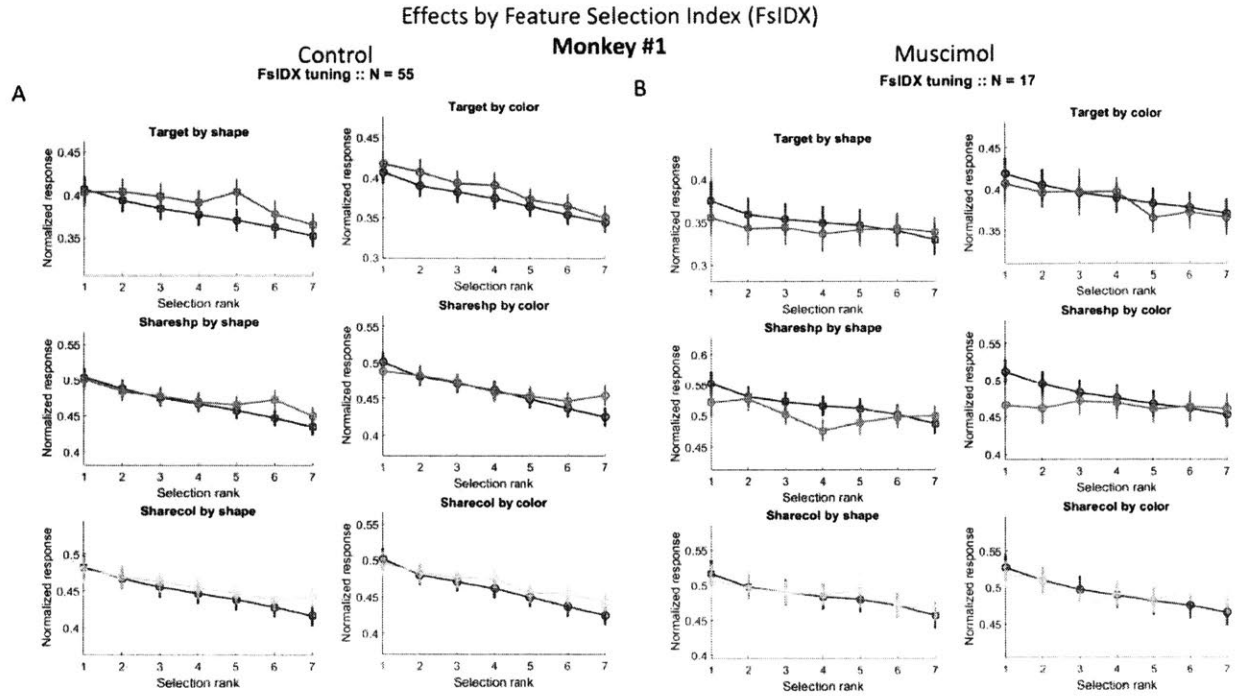

Figure 8.

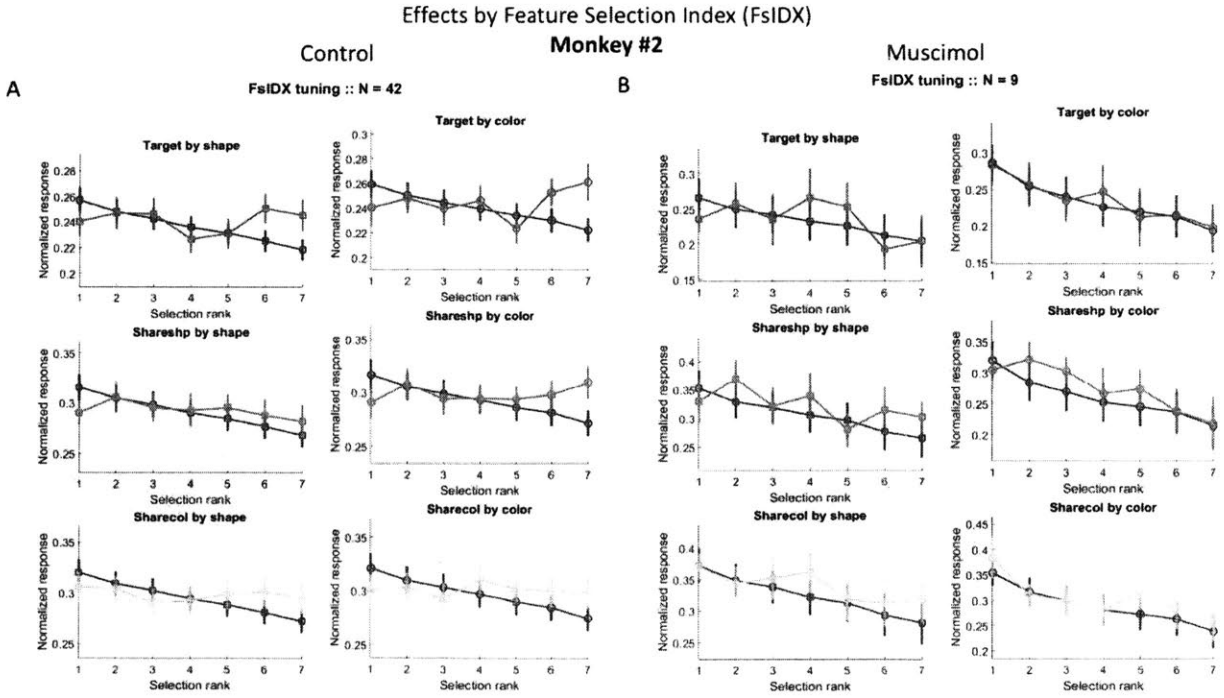

Figure 9.

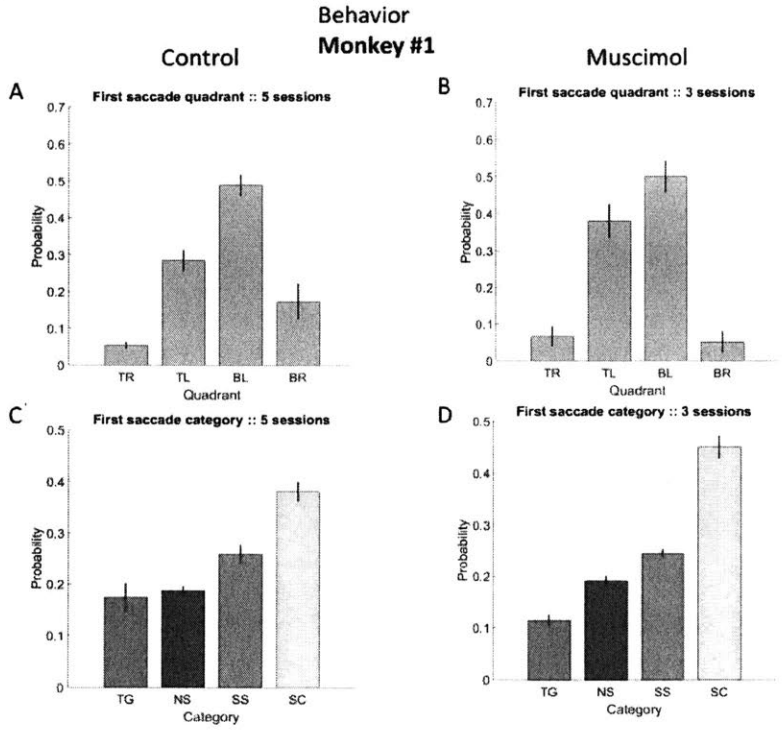

Figure 10.

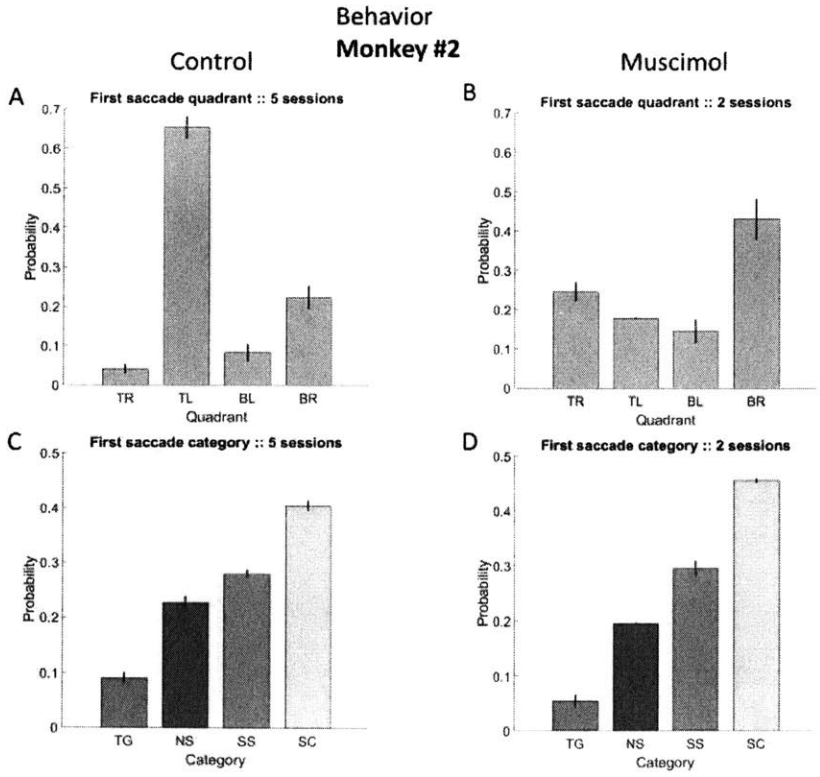

SUPPLEMENTARY FIGURES

Supplementary Figure 1.

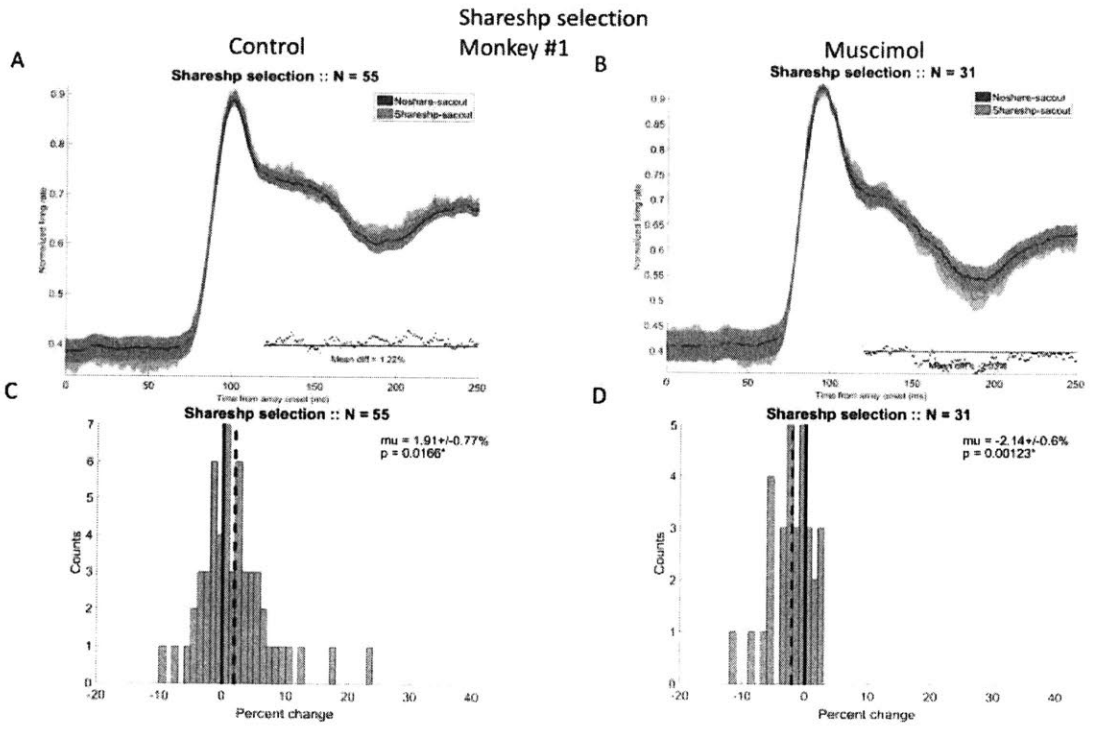

Supplementary Figure 2.

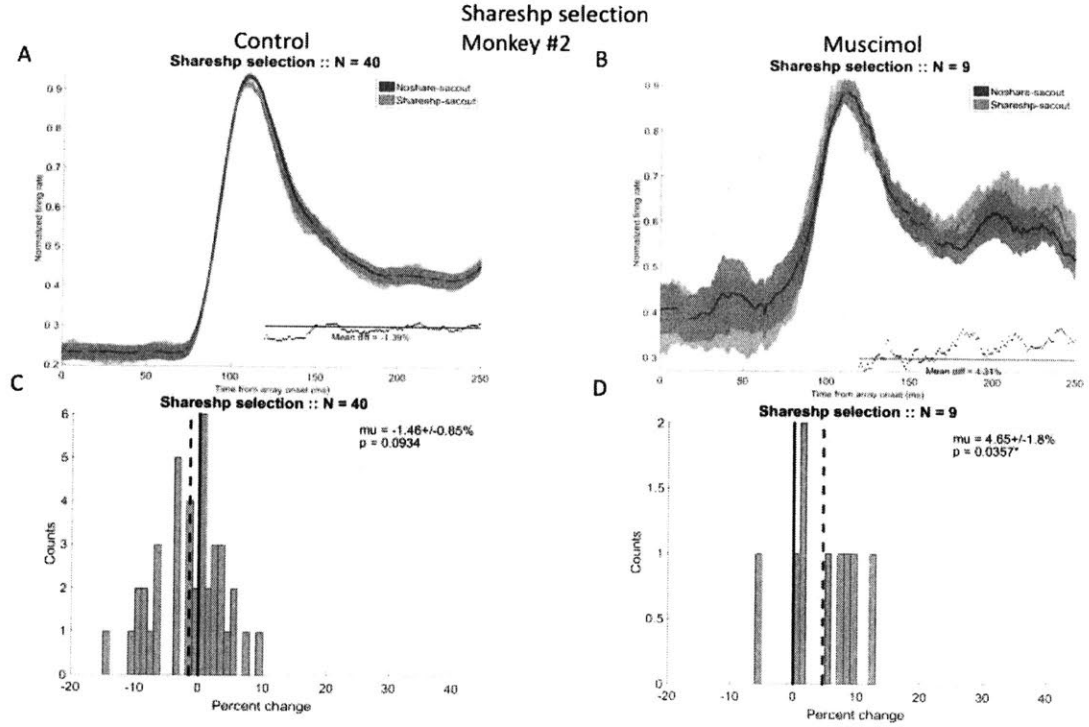

Supplementary Figure 3.

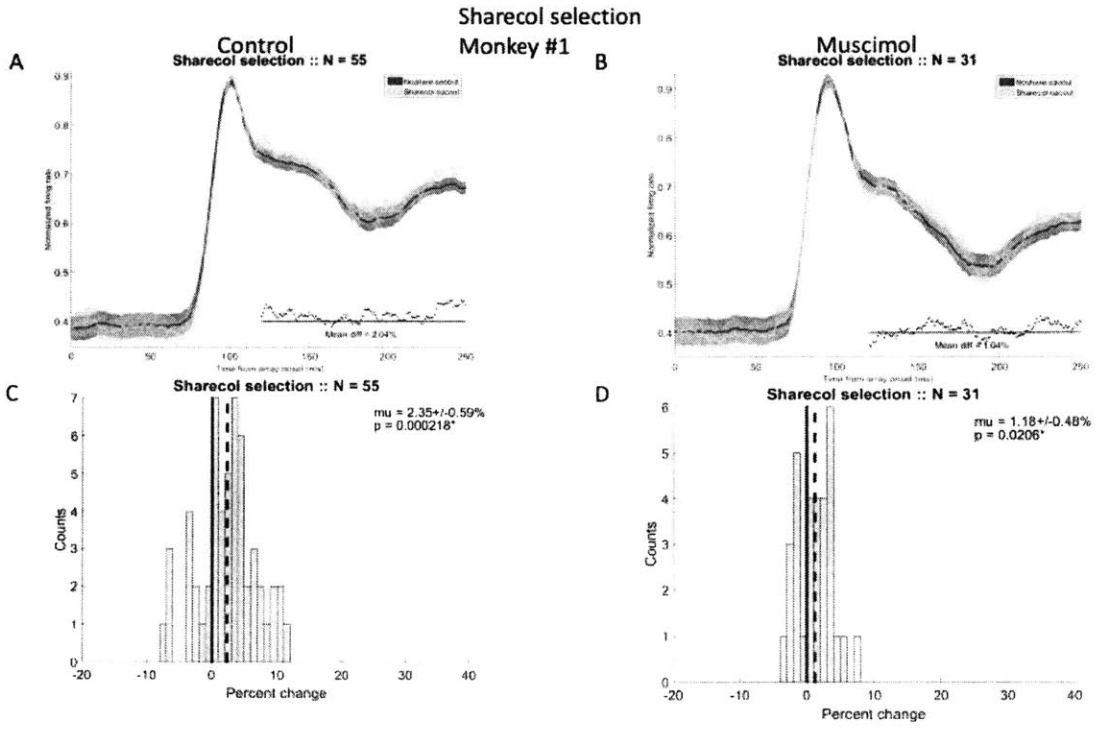

Supplementary Figure 4.

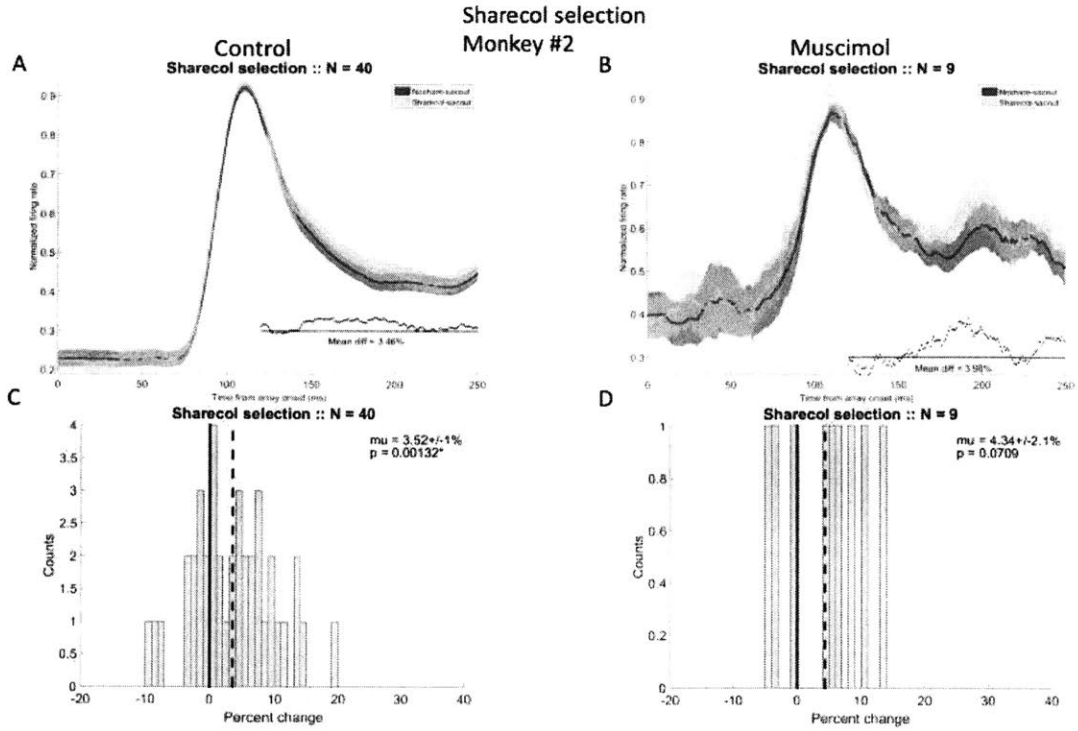

Supplementary Figure 5.

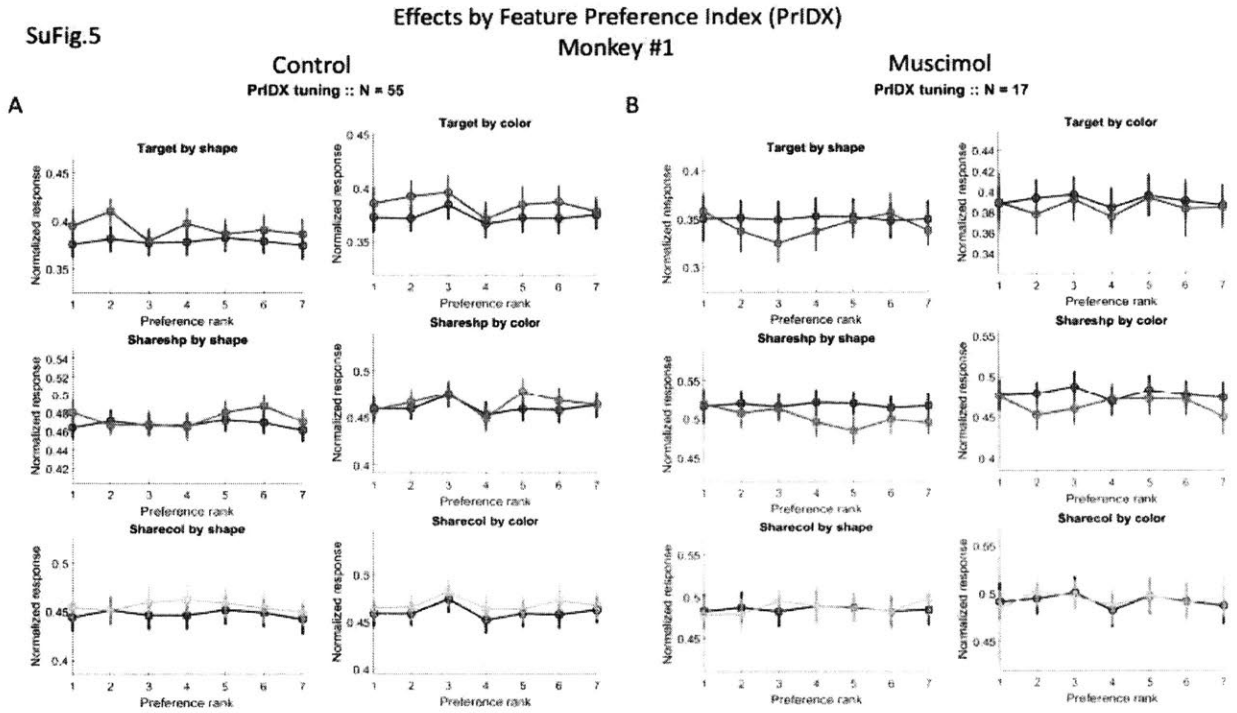

Supplementary Figure 6.

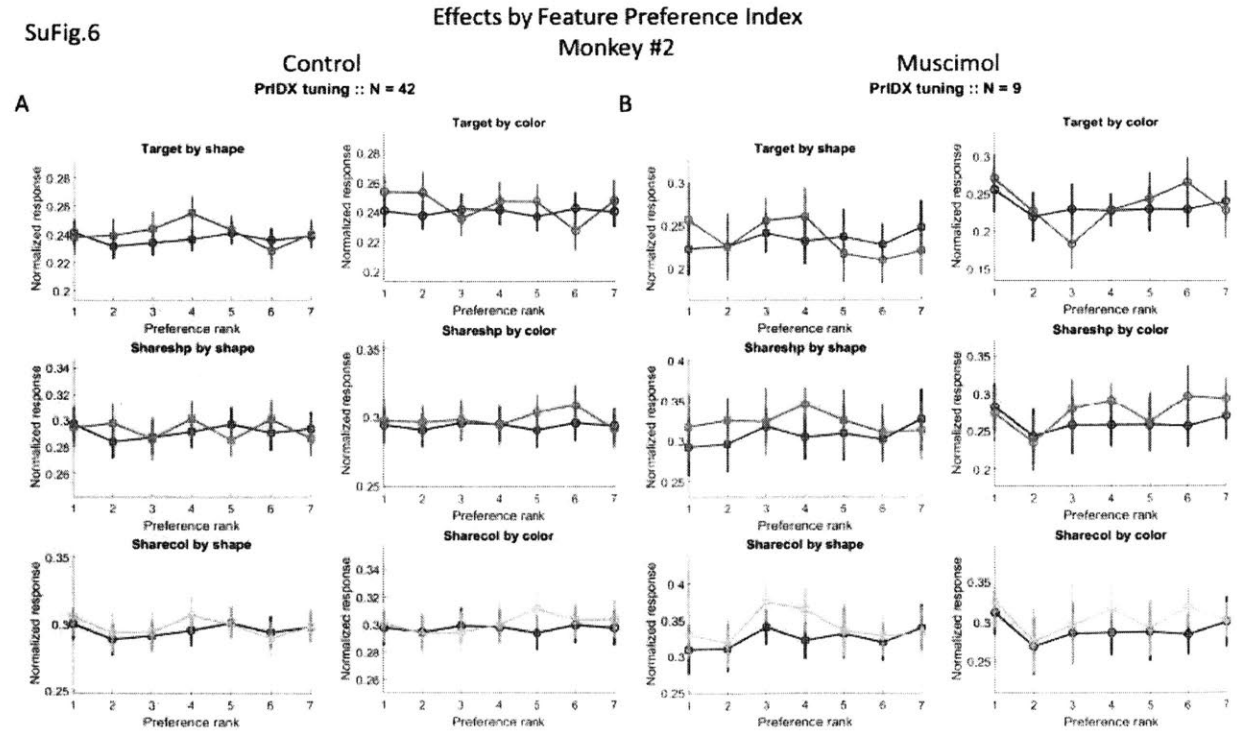

Supplementary Figure 7.

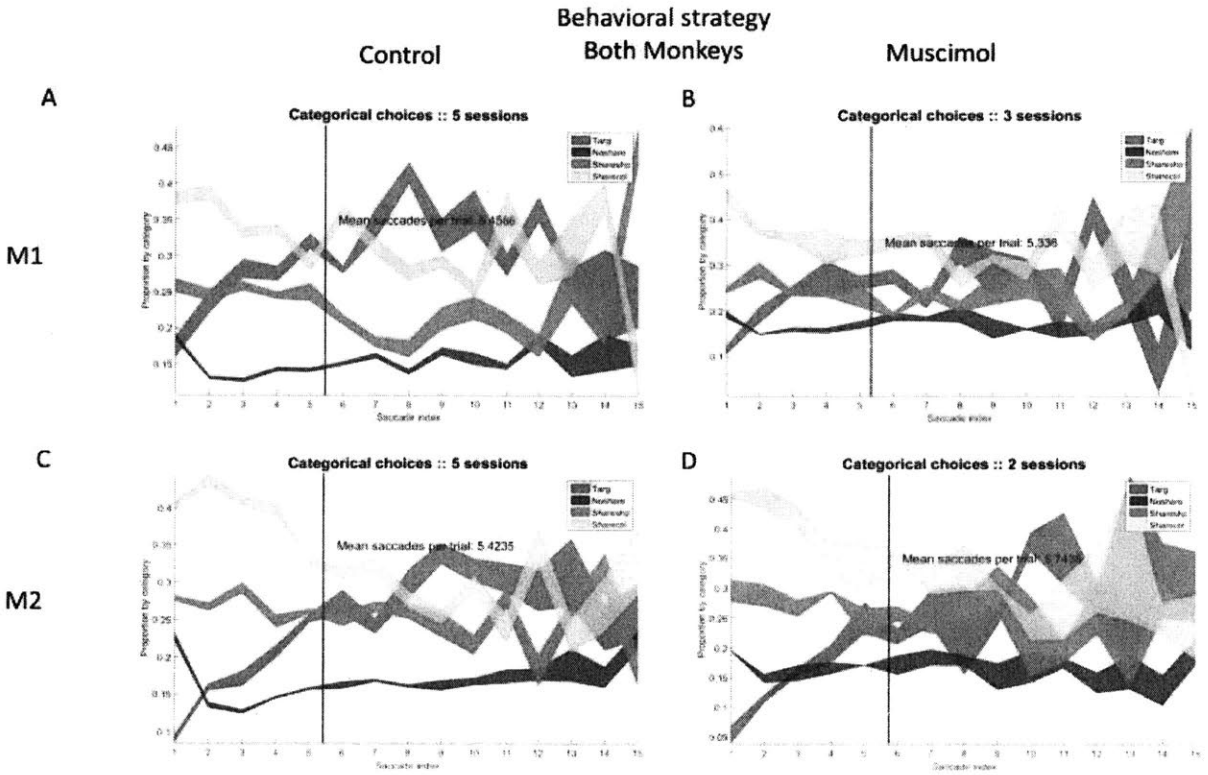

Supplementary Figure 8.

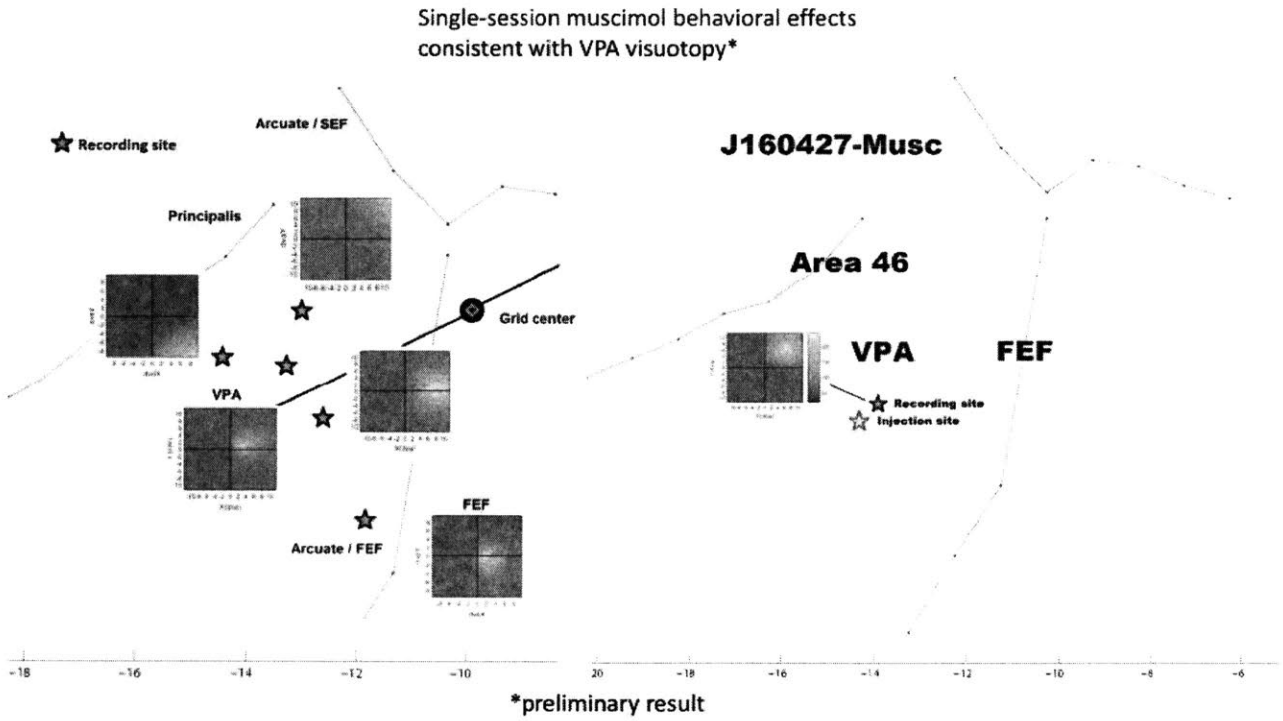

Supplementary Figure 9.

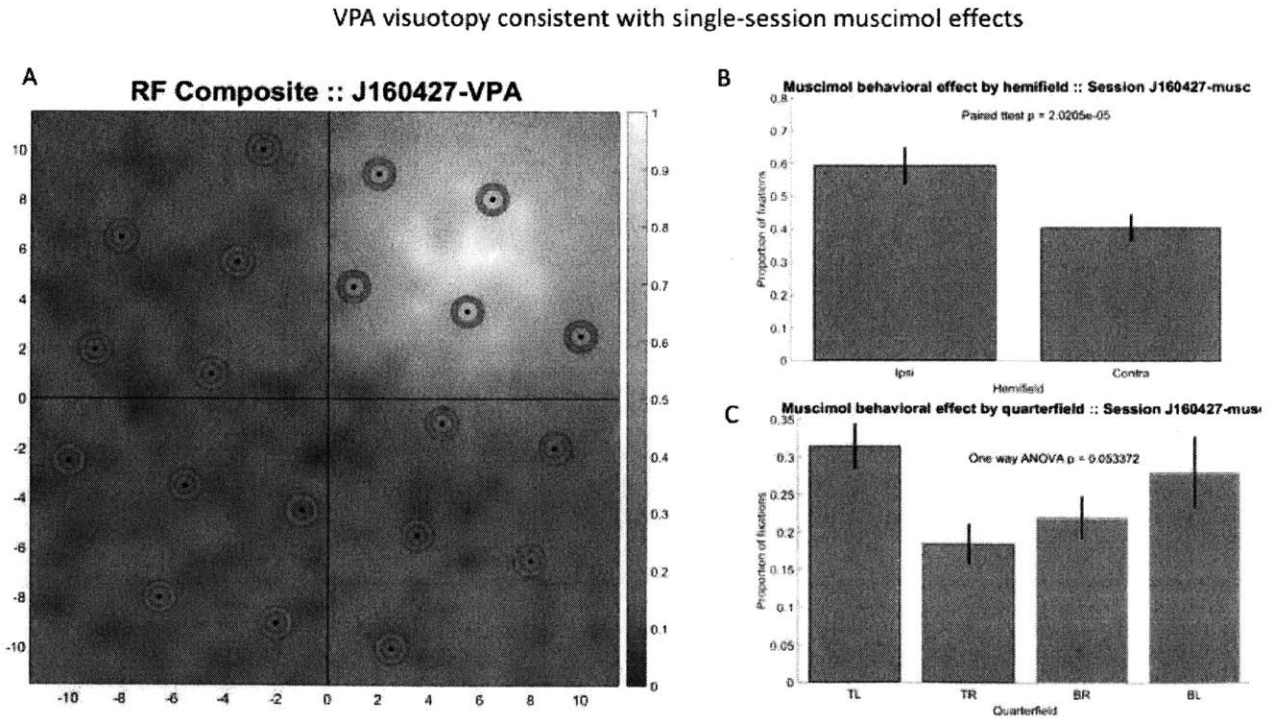

Supplementary Figure 10.

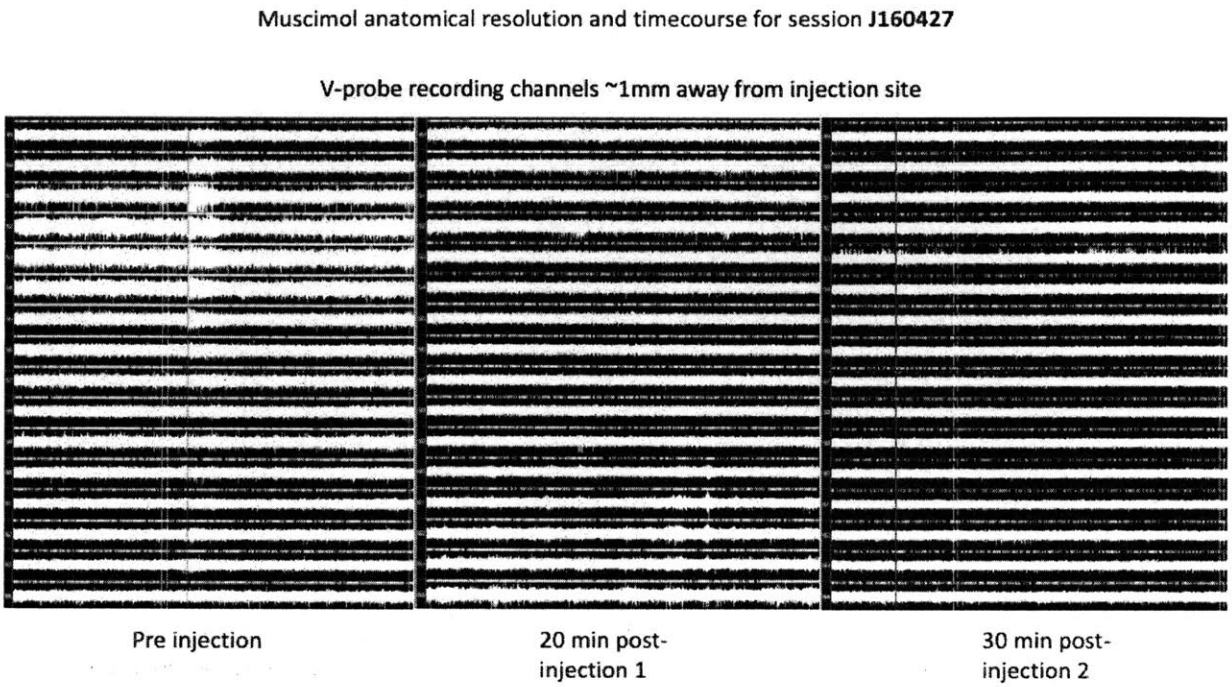

Supplementary Figure 11.